

SMALL-FOOTPRINT DISCRETE-RETURN LIDAR IN TREE SPECIES RECOGNITION

I. Korpela ^a, T. Tokola ^a, H. O. Ørka ^b, M. Koskinen ^a

^a Dept. of Forest Resource Management, POB 27, 00014 University of Helsinki, Finland

^b Dept. of Ecology and Natural Resource Management, Norwegian University of Life Sciences, POB 5003, N-1432 Ås, Norway – ilkka.korpela@helsinki.fi

Commission VII

KEY WORDS: Airborne laser scanning, Single tree, Intensity, Classification, Monoplotting, Crown modeling.

ABSTRACT:

In forest inventories, the species information is crucial for economical, ecological and technical reasons. Species recognition is currently a bottleneck in practical remote sensing applications. Here, we examined species discrimination using tree-level LiDAR features in discrete-return data. The aim was to examine the robustness and explanatory power of the intensity and height distribution features. A dataset consisting of 13890 trees from 117 stands in southern Finland (61°50'N, 24°20'E) was used. The data of two LiDAR sensors was fused using intensity normalization in natural targets. Age dependency of first-return intensity was observed in spruce and birch trees, which needs to be considered in using LiDAR intensity metrics. Classification of Scots pine, Norway spruce and birch was tested and accuracy was 81–85%. Separation of pine and spruce was more accurate, 91–93%. We also present results for 15 rare conifer and broadleaved species. To enhance the classification accuracy of birch, we propose co-use of image features.

1. INTRODUCTION

1.1 LiDAR in forest inventories

The conventional way of measuring trees is giving way to new applications, which combine *in situ* observations and remote sensing data. The introduction of airborne laser scanning was a breakthrough as it allows for accurate 3D probing of the vegetation and terrain (Næsset 2004, Packalén and Maltamo 2007). Before LiDAR, automated 3D methods were never tried in practice although method development in image matching for canopy surface modeling and for 3D treetop positioning was active (Miller et al. 2000, Korpela 2004, 2007).

Since 2002–2006, in Scandinavia, LiDAR is has been applied by companies mainly for area-based but also for single-tree remote sensing (STRS). As the names imply, the two differ in the used unit of observation. Trees constitute distinct targets, but STRS requires a high sampling density and individual trees are not always detectable. The accuracy at tree level is restricted by the imprecision of allometric relationships between the measurable tree dimensions and the variables of interest. For example, in Finnish trees, the best attainable RMS-accuracy for stem diameter is 10% (Korpela and Tokola 2006) and tree positions have a planimetric accuracy of 0.2–0.4 m (Korpela et al. 2007b). In area-based remote sensing, the forest is characterized by features that are computed from the LiDAR point cloud. The features measure the vertical structure and density of the canopy and the species mixture and are correlated with forest parameters that are of interest to the foresters. A training set comprising of field samples, the reference plots, is used in the estimation of imputation models, which are applied in areas where *in situ* data is missing. As in supervised learning, the accuracy of the results depends on the quality of the training data and the dependencies between the forest parameters and the LiDAR features. If tree positions are not preferred and stand-level volume/biomass estimates are vital, the area-based technique may well be more cost-efficient in practical forest inventories. The accuracy of per-species data has improved recently with the co-use of LiDAR and images (Packalén and Maltamo 2007).

1.2 Tree species identification in images and LiDAR

In forest inventories, the species information is crucial for economical, ecological and technical reasons. Errors made in the species can cause prominent bias in the estimates of tree biomass, because the allometric dependencies (canopy properties predict stems) that are modeled with the LiDAR features are species-specific.

In Finland, there are four commercially important species, which constitute over 98% of the stem volume. These are Scots pine (*Pinus sylvestris* L.), Norway spruce (*Picea abies* (L.) H. Karst.), birch (*Betula pubescens* Ehrh., *Betula pendula* Roth.) and aspen (*Populus tremula* L.). Aspen is a rare species of the best sites. In automated image-based species identification, the separation between pine and spruce has proven difficult (60–70% accuracy) because of the overlap of spectral features (Haara and Haarala 2002). Structure-based classification in which the branching patterns are used requires very-high resolution near-nadir data, which is accurate, but leads to high data costs (Brandtberg 1999). Korpela (2004) used photogrammetric 3D treetop positioning followed by image-based crown modeling which allowed for the sampling of spectral values in several images. The features that characterized self-shading in a crown enhanced the identification accuracy of pine, spruce and birch to 85%.

LiDAR data offers a complement to optical data. Single-tree species recognition from 1–4-return LiDAR data was studied by Brandtberg et al. (2003), Holmgren and Persson (2004), Brandtberg (2007) and Ørka et al. (2007). Flying heights of 100–750 m and footprint diameters 10–20 cm were reported. Both geometric and intensity features were tested. Holmgren and Persson (2004) extracted LiDAR points within a crown and computed 20 features. They achieved an accuracy of 95% in separating 562 samples of pine and spruce. Crown base height, variation of intensity and the mean intensity of returns near the estimated crown surface were the strongest features. Brandtberg (2007) provides an elaborate discussion of the LiDAR-crown interactions. He obtained an accuracy of 64% in

the classification of three broad-leaved species in West Virginia using height and intensity distribution metrics. Ørka et al. (2007) examined species identification in south Norway for 224 samples of Birch, aspen and Norway spruce. The LiDAR data was divided according the echo-type, first-only-last, and the per-tree mean and standard deviation of intensity were computed for the three echo-types. The accuracy varied from 60 % to 74 % depending on the number of variables. Coniferous and deciduous trees differ in NIR-reflectance in optical but, Ørka et al. (2007) did not observe notable differences in the intensity of the LiDAR at $\lambda=1064$ nm. Co-use of LiDAR intensity in species classification in young seedling stands was examined by Korpela et al. (2008). Intensity provided an aid in the detection of the competing vegetation, but the accuracy in the separation of coniferous and broad-leaved, 0–4-m-high trees was only moderate. In older trees, combination of optical data with LiDAR improved the species classification results (Heinzel et al. 2008, Persson et al. 2004).

The use of full-waveform LiDAR for tree detection and species identification was examined by Reitberger et al. (2006, 2008) and Höfle et al. (2008). Litkey et al. (2007) provide interesting examples of waveforms superimposed in terrestrial close-range images. Waveform data allows for a more detailed description of the echo. Also, an increase in point density is achieved by the decomposition of waveforms (Wagner et al. 2006), which is beneficial in tree detection and increases the structural details that can be used for species determination (Reitberger 2008). Echo width and amplitude (~intensity) have been used to characterize tree species. Höfle et al. (2008) used calibrated full waveform data for species discrimination of European larch (*Larix decidua* Mill.), oaks (*Quercus robur* L., *Q. petraea* (Matt.) Liebl.) and Beech (*Fagus sylvatica* L.). Echo width separated larch from the broad-leaved trees, but oak and beech showed a similar response in backscatter cross-section and echo width.

In addition to LiDAR systems parameters, the scanning range and the atmospheric losses, echo width and amplitude/intensity are affected by the illuminated area, the BRDF of the illuminated targets and the incidence angles i.e. the target geometry (Höfle et al. 2008). This means that retrieval of reflectance of tree canopies is ill-posed even in radiometrically calibrated data and the radiometric LiDAR parameters will exhibit substantial intraclass (tree/segment-level) variation. This in turn means that species determination has to be based on the analysis of distribution characteristics that are derived from a multitude of pulses that have interacted with the tree under investigation.

1.3 Objectives

Our aim was to study assess the usability of tree-level features in discrete-return LiDAR data for tree species classification and to examine factors that potentially influence the species-specific intensity signatures and needs thus consideration in the use of LiDAR data for species determination. A substantial data set consisting of 13890 trees was compiled to allow the detection of these effects.

2. METHODS

2.1 Study area, reference trees and LiDAR

The experiment was carried out near the Hyytiälä forest station in southern Finland (61°50'N, 24°20'E). Rotation ages are 75–120 yrs and trees attain a height of 24–33 m. Scots pine and Norway spruce dominate and form both mixed and pure stands. Birch stands are all younger than 40 years, because of the past silviculture. Isolated birches occur in older coniferous stands. Mineral soils with gentle slopes prevail and the elevation is 135–198 m. Lakes, open mires, spruce mires and pine bogs cover the basins. The mires are largely drained. The study area extends 2×6 km, and encompass a multitude of permanent forest plots both in managed and pristine forests, on mineral soils and in both pristine and drained peatland. The area is covered by aerial photographs of 1946–2008 and four LiDAR campaigns in 2004–2008. We used LiDAR data from 2006 and 2007 (Table 1). Both campaigns had a density of 6–8 pulses per m².

Instrument	ALTM3100	ALS50-II
Date	July 25, 2006	July 4, 2007
Pulse frequency	100 kHz	115.8 kHz
Scan frequency	70 Hz	52 Hz
Footprint	25–28 cm	17–18 cm
Range	840–950 m	770–820 m
Scan angle	± 14°	± 15°
Air humidity, 2 m	48–52%	60–75%
AGC	-	8 bits

Table 1. Characteristics of the LiDAR datasets.

Both LiDAR datasets were normalized for the range. ALS50-data was also compensated for the influence of the automatic gain control (Korpela 2008). In addition, the range and AGC-normalized intensity values of ALS50 were further normalized to match the ALTM3100 data by a simple multiplication. Natural targets including gravel, asphalt, an oat field, grass, ground lichens and shrubs were used for finding the normalization parameters. It is possible that the AGC-compensation in ALS50 was ineffective for some sites near forest-lake (low intensity – fluctuating reflections) or forest-field (high intensity) margins, where the AGC-changes were abrupt. Also, due to the AGC, the ALS50 8-bit intensity data was saturated in some non-forest areas. In the analysis the data of the two sensors were fused.

Over 15000 reference trees have accumulated in field measurement campaigns during 2002–2008 organized by the first author. Before 2006, a tacheometer was used for the mapping of trees. In 2006–2008, a photogrammetric-geodetic mapping procedure was applied (Korpela et al. 2007a). In it, the photo-visible trees are first positioned using ray-intersection in multiple aerial images or by a monoplotting procedure that employs the LiDAR point cloud (Figure 1). The photo-trees serve a control points in the field and small trees are positioned using trilateration and triangulation. Trees in young stands with heights of below 6 m were mapped using Network RTK. All trees were recorded for species, stem diameter and crown status. The proportion of trees that were measured for the depth of the living crown and tree height has varied from 30% to 100%. All field plots are fixed-area plots, circular, rectangular or free in shape and 0.1–1.8 ha in size. In 2002, crown width was additionally measured in nearly 1000 trees. To study the response of rare tree species in LiDAR intensity,

580 semi-urban trees were mapped in August 2007 near the Hyttiälä forest station (arboretum, forested farmland, garden forests, forest margins, lake shores, open grown trees) on fertile soil. Domestic and exotic species included alder (*Alnus glutinosa* (L.) Gaertner), grey alder (*Alnus incana* (L.) Moench), Goat willow (*Salix caprea* L.), Norway maple (*Acer platanoides* L.), Siberian larch (*Larix sibirica* Ledeb.), rowan (*Sorbus aucuparia* L.), Douglas fir (*Pseudotsuga menziesii* (Mirb.) Franco) and Siberian fir (*Abies sibirica* Ledeb.).

All trees were visually verified to exist at the time of the LiDAR campaigns using aerial images of August 2006 and June 2007, and the treetop position was re-measured using the monoplotted technique (Figure 1.) Some broken, fallen or cut trees were rejected. Trees that were discernible in the images and LiDAR data were included. Most trees with a relative height of below 50% were thus rejected because they were not seen in the images and the point cloud. The unseen trees constitute 0–10% of the stem volume and commercial value and this proportion depends on the height variation and density of the stand (Korpela 2004).

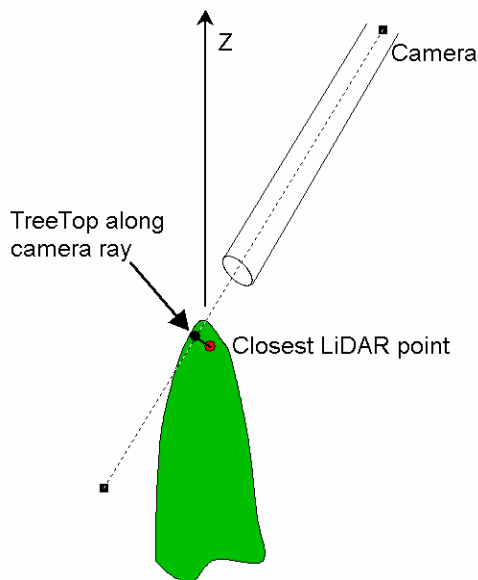


Figure 1. Principle of the monoplotted method used for treetop positioning. The treetop is positioned in one image by the operator (usually the back-lit case) and the distance to the first LiDAR point intersected by the camera ray (width 0.5–1 m) is used for the treetop position. In fused LiDAR data with 12–18 pulses per m², the mean underestimation of Z was 0.33 m in 465 trees measured in the field in 2007.

2.2 Extraction of LiDAR features

Extraction of LiDAR data and features for the reference trees was automated using a crown modeling procedure. The objective was to, as accurately as possible; collect the LiDAR points that belong to each tree. In a dense forest where crowns are interlaced, this is an ill-posed task, and some noise will remain in the per tree data, especially in the lower part of the crown where the branches of neighboring trees overlap. Figure 2 illustrates the problem. First, field measurements of crown width (n=871) were used for estimating regression models that predict the crown width using species, stem diameter and tree height as predictors. The regression estimate of crown width

was increased 0–20%, depending on stand density, and this estimate provided an initial approximation for the maximal crown width. It was applied in an iterative adjustment of a crown model. A three-parameter curve of revolution was fitted to the LiDAR point cloud (Korpela et al. 2007b). Weighted least square adjustment was used in the parameter estimation. In it, LiDAR points, observations of crown radius, outside the crown envelope are weighted by a factor five as weighting improves the fit to the real crown extent. The length of the crown model was 40% down from the top. This is a coarse approximation. For example, young and open-grown spruce trees have deeper crowns. LiDAR points inside or near the modeled crown (within one RMSE), were included. In 2.5% of the cases the iteration failed and these trees were excluded. The features computed using the points are in Table 2.

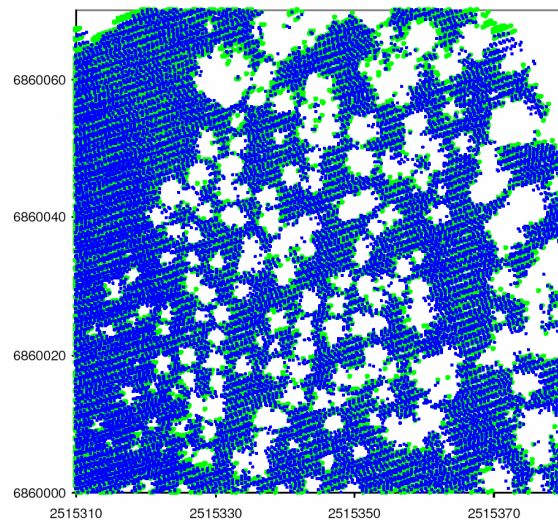


Figure 2. Map of LiDAR pulses that have echoed from a height of below 20 m have been back-projected to a mapping surface 20 m above the DEM. The map is from a 25–30-m-high spruce stand. The large openings in the periphery are caused by big pine and birch crowns. The green dots represent ALTM3100 and blue dots are ALS50 'echoes'. Data from 6 strips is seen. The XY-match is reasonable.

Feature	Description
<i>im, isd</i>	Mean and SD of intensity
<i>imsurf, isdsurf</i>	As above, but <0.3 m from the envelope
<i>id1–id10</i>	Deciles of the intensity distribution
<i>hd1–hd10</i>	Deciles of the relative height distribution
<i>iMin</i>	Minimum intensity (<i>id10 = IMax</i>)
<i>iq1–iq4</i>	Mean intensity 0–10%, 10–20%, 20–30%, 30–40% down the top
<i>iq12, iq13, iq14</i>	Transformations <i>iq1/iq2, iq1/iq3, iq1/iq4</i>

Table 2. Features derived from the LiDAR data assigned to a tree. Intensity features were computed using first-return data only. *hd* features make use of all points.

2.3 Classification method

The non-parametric k-NN method was applied with leave-one-out cross-validation. Feature selection was based on visual assessment of Box-Whisker plots, correlation analysis and ANOVA of the individual features. Performance measures were the overall classification accuracy and the simple Kappa.

3. RESULTS

3.1 Examination of individual features

There were differences in the mean intensity of first-return points in 20–135-yr-old pine, birch and birch trees (Table 3).

	Pine, n=5007		Spruce, n=6120		Birch, n=1979	
<i>im</i>	37.3	5.1	45.5	5.9	52.6	10.1
<i>isd</i>	16.0	2.2	19.1	2.2	20.2	3.6

Table 3. Mean and SD of features *im* and *isd*. Living pine, spruce and birch trees.

The LiDAR features *imsurf* and *isdsurf* that were derived using the crown surface points showed very high correlation with features *im* and *imsurf*. Given the errors in the crown model estimation and the planimetric imprecision of the LiDAR (~0.2 m), this analysis was unable to detect horizontal intensity differences.

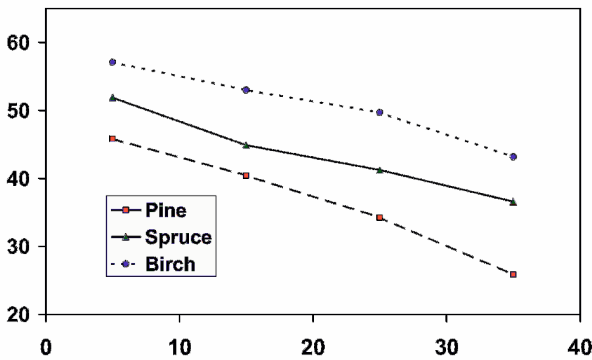


Figure 3. Mean intensity values at relative heights of 0–10%, 10–20%, 20–30% and 30–40% down from the top for 20–135-yr-old pine, spruce and birch trees.

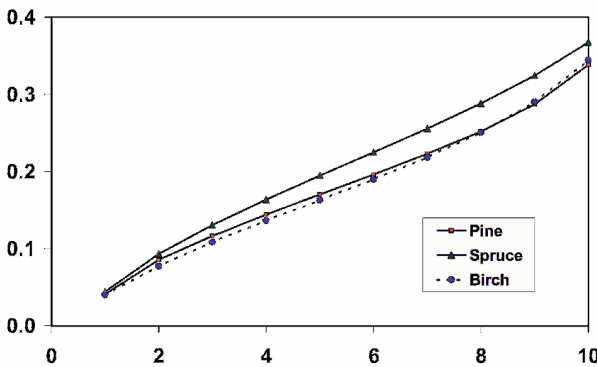


Figure 4. Height deciles, *hd1–hd10* for living pine, spruce and birch trees.

In the first-return data, intensity values were highest near the tree top and decreased downwards (Figure 3). The most probable explanation is that the leaf/needle density in shoots decreases downwards as the light environment worsens for the shaded shoots in a tree. However, it cannot be excluded that dampening of intensity is due to transmission losses in the canopy, which attenuate the signal. It was interesting to note that the response in *im* was different for trees of varying age (Figs. 5–7). It can be explained by changes in the crown architecture, in the foliage/needle density and/or changes in the

reflectance of the LiDAR-illuminated scatterers. Birch and spruce showed an age-dependency in the mean intensity. In 20–30-m-high birches, the intensity was 20–30% lower compared to young trees. The foliage mass and its vertical and horizontal distribution in an individual tree are influenced by many factors that include tree spacing, site fertility, fertilization, insect damages, age and growth rate. For example, the branching pattern, even the shape of needles in old pine and spruce trees differs notably from the young and vigorous trees (Stenberg et al. 1999). This may explain as to why the intensity was higher in the old, 25–33-m-high pines with a round-shaped crown. In old pines, the top branches get thicker and the crown becomes more of a level surface than a cone. The bare, thick, densely packed branches can probably result in a higher intensity. In less-light conditions, down the canopy, the needles tend to be broad and flat, whereas the so-called sun-needles are more cylindrical in shape (Stenberg et al. 1999). Also, needle density is lower in the bottom of canopy (Cermák et al. 1998), and shoots tend to be more vertical than in the top part (Stenberg et al. 1994). Birch trees have widespread crowns and the foliage-density per unit area, or the depth of the leaf-layer possibly diminishes for older trees.

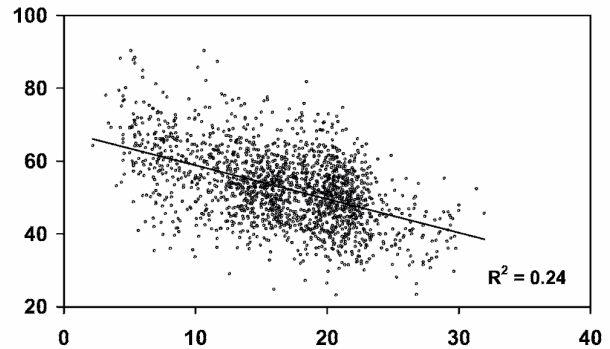


Figure 5. *im* × tree height in 20–135-yr-old birches (n=1979).

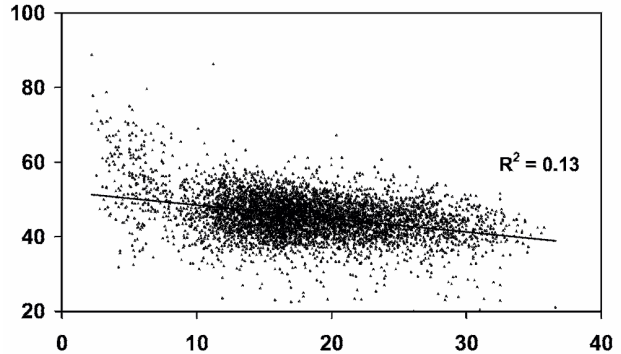


Figure 6. *im* × tree height in 20–135-yr-old spruces (n=6120).

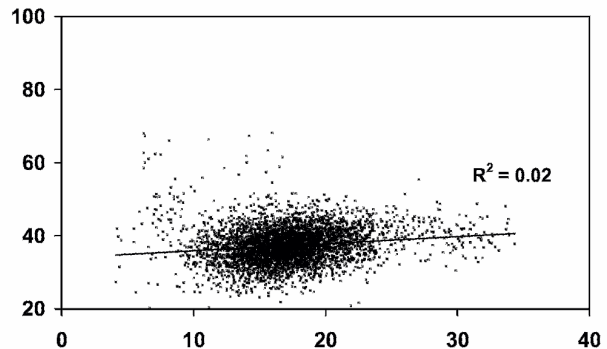


Figure 7. *im* × tree height in 20–135-yr-old pines (n=5007).

3.2 Classification of pine, spruce and birch

Using a set of 12933, 20-135-yr-old trees from diverse site conditions, and ten explanatory variables $\{im, isd, iql, iql2, iql3, iq3, iq4, hd2/hd8, hd5\}$ with leave-one-out cross-validation in k-NN, an overall classification accuracy of 81% was achieved (Table 4) for pine (89%), spruce (78%) and birch (72%).

	Pine	Spruce	Birch	All
Pine	4429	403	165	4997
Spruce	349	4671	1003	6023
Birch	100	434	1379	1913
All	4878	5508	2547	12933

Table 4. Confusion matrix of k-NN classification. Kappa=0.69.

If birch was excluded, the accuracy was 92% ($\kappa=0.84$) for pine and spruce. In young trees, height of below 18 m ($n=7307$), the accuracy improved to 82% and 93% ($\kappa=0.86$) for the 3-class and binary cases, respectively. In the old trees, the accuracies were 85% and 91%. Birch and spruce were confused in 20–25% of the cases. Separation of was more reliable in the older stands. The discrimination of pine and spruce was very reliable, with accuracies above 90%.

3.3 Rare and exotic species

Norway maple has large leaves that form a relatively shallow layer on the crown envelope. The mean intensity (im) was highest in maple (Table 5). The shoot structure of goat willow gives raise to high intensity. The leaf normal is upright and the leaves form surfaces that cover the shoot. Siberian fir had the highest intensity in conifers, which is also explained the structure of the shoots and needles that form dense planar mats. In the family of Birch trees, alder had the highest intensity. Again, the leaf inclination angle of alders (*Alnus* sp.) and birch (*Betula* sp.) is different. The semi-urban pines and spruce trees did not show any difference in intensity and aspen mixes with birch (Table 5).

Species	n	Mean	SD
Norway Maple	30	72.1	11.0
Goat willow	66	66.5	11.2
Rowan	32	66.0	13.8
Siberian fir	45	64.5	9.2
Small-leaved lime	9	59.5	8.1
Alder	89	57.2	11.1
Siberian larch	17	56.9	9.6
Grey alder	16	53.9	11.0
Douglas fir	2	53.4	3.3
Wych elm	7	52.3	7.3
Cembra pine	9	51.4	5.1
Aspen	64	49.9	11.3
Birch	100	45.3	10.9
Spruce	32	44.3	5.8
Pine	38	43.9	6.3
Contorta pine	2	37.9	4.9

Table 5. Mean intensity (im) in trees in the vicinity of the Hyttiälä forest station. 50% of birch and all maple samples represent open-grown trees.

4. DISCUSSION

The potential use of intensity and height distribution variables in small-footprint discrete-return LiDAR data for tree species discrimination were tried with 13890 trees from 117 forests stands. The results apply to 20–135-yr-old, intermediate, co-dominant and dominant trees. Suppressed trees, with relative height of below 50% were not included here.

LiDAR data of two sensors were fused in the analyses by normalizing the intensities. The imperfections of the fusion probably caused additional noise in the intensity data and impaired the results.

The analysis omitted factors such as the site fertility and treatment history, which may affect foliage patterns in trees. These we will examined in the future, since they may exercise an effect on the species-specific signatures and need to be observed in the selection of training data and imputation models.

Here, the LiDAR echoes belonging to a particular tree were carefully selected using field measurements that predicted crown dimensions. We will further analyze if the errors of species classification can be explained by the relative size of the tree and by the spatial pattern of the neighbors, because the labeling of the LiDAR echoes in a dense canopy is ill-posed.

The accuracy of above 90% for the separation of pine and spruce is promising, and the results were obtained with 11000 trees representing a wide range of growing conditions. Separation of birch from spruce most likely requires the use of optical data. With LiDAR only, the accuracy was restricted to 80–85%. We will test the co-use of image features derived from UltraCAM D and ADS40-SH52 data for the trees used here. Optical data will be an aid in the classification of dominant and co-dominant trees that are seen in direct light.

5. REFERENCES

- Brandtberg, T., 1999. Automatic individual tree based analysis of high spatial resolution aerial images on naturally regenerated boreal forests. *Canadian Journal of Forest Research*, 29, pp. 1464-1478
- Brandtberg, T., Warner, T.A., Landerberger, R.E, McGraw, J.B., 2003. Detection and analysis of individual leaf-off tree crowns in small footprint, high sampling density lidar data from the eastern deciduous forest in North America. *Remote Sensing of Environment*, 85, pp. 290-303
- Brandtberg, T., 2007. Classifying individual tree species under leaf-off and leaf-on conditions using airborne lidar. *ISPRS Journal of Photogrammetry & Remote Sensing*, 61, pp. 325–340
- Cermák, J., Riguzzi, F., Coulemans, R., 1998. Scaling up from the individual tree to the stand level in Scots pine. I. Needle distribution, overall crown and root geometry. *Annals of Forest Science*, 55, pp. 63-88.
- Haara, A., Haarala, M., 2002. Tree species classification using semi-automatic delineation of trees on aerial images. *Scandinavian Journal of Forest Research*, 17, pp. 556–565.

- Heinzel, J. N., Weinacker, H., Koch, B., 2008. Full automatic detection of tree species based on delineated single tree crowns - a data fusion approach for airborne laser scanning data and aerial photographs. *Proceedings of SilviLaser 2008*, Edinburgh, UK, pp. 76-85.
- Holmgren, J., Persson, Å., 2004. Identifying species of individual trees using airborne laser scanner. *Remote Sensing of Environment*, 90, pp. 415-423.
- Höfle, B., Hollaus, M., Lehner, H., Pfeifer, N., Wagner, W., 2008. Area-based parameterization of forest structure using full-waveform airborne laser scanning data. *Proceedings of SilviLaser 2008*, Edinburgh, UK, pp. 227-236.
- Korpela, I., 2004. Individual tree measurements by means of digital aerial photogrammetry. *Silva Fennica Monographs*, 3, pp. 1-93.
- Korpela, I., 2007. 3D treetop positioning by multiple image matching of aerial images in a 3D search volume bounded by lidar surface models. *Photogrammetrie, Fernerkundung, Geoinformation*, 1/2007, pp. 35-44.
- Korpela, I., 2008. Mapping of understory lichens with airborne discrete-return LiDAR data. *Remote Sensing of Environment*, 112(10), pp. 3891-3897
- Korpela, I., Tokola, T., 2006. Potential of aerial image-based monoscopic and multiview single-tree forest inventory - a simulation approach. *Forest Science* 52(3), pp. 136-147
- Korpela, I., Välimäki E., Tuomola, T., 2007a. Mapping forest plots: An efficient method combining photogrammetry and field triangulation. *Silva Fennica*, 41(3), pp. 457-469
- Korpela, I., Dahlin, B., Schäfer, H., Bruun, E., Haapaniemi, F., Honkasalo, J., Ilvesniemi, S., Kuutti, V., Linkosalmi, M., Mustonen, J., Salo, M., Suomi, O., Virtanen, H., 2007b. Single-tree forest inventory using LiDAR and aerial images for 3D treetop positioning, species recognition, height and crown width estimation. *IAPRS Volume XXXVI*, Part 3/W52, pp. 227-233
- Korpela I., Tuomola T., Tokola T., Dahlin, B., 2008. Appraisal of seedling stand vegetation with airborne imagery and discrete-return LiDAR – an exploratory analysis. *Silva Fennica*, 42(5), pp. 753-772.
- Litkey, P., Rönnholm, P., Lumme, J. Liang, X., 2007. Waveform features for tree identification. *IAPRS, Volume XXXVI* part 3/W52, pp. 258-263.
- Ørka, H. O., Næsset, E., Bollandsås, O. M., 2007. Utilizing airborne laser intensity for tree species classification. *IAPRS Volume XXXVI*, Part 3/W52, pp. 300-304
- Miller, D., Quine, C., Hadley, W., 2000. An investigation of the potential of digital photogrammetry to provide measurements of forest characteristics and abiotic damage. *Forest Ecology and Management*, 135, pp. 279-288.
- Naesset, E., 2004. Practical large-scale forest stand inventory using a small-footprint airborne scanning laser. *Scandinavian Journal of Forest Research*, 19(2), pp. 164-179.
- Packalén, P., Maltamo, M., 2007. The k-MSN method for the prediction of species-specific stand attributes using airborne laser scanning and aerial photographs. *Remote Sensing of Environment* 109, pp. 328-341.
- Persson, Å., Holmgren, J., Södermann, U., Olsson, H., 2004. Tree species classification of individual trees in Sweden by combining high resolution laser data with high resolution near-infrared digital images. *IAPRS, Volume XXXVI*, Part 8/W2. 4 p.
- Reitberger, J., Krzystek, P., Stilla, U., 2006. Analysis of full waveform LiDAR data for tree species classification. *IAPRS, Volume XXXVI, ISPRS symposium PCV'06*, ISSN 1682-1750, pp. 228-233.
- Reitberger, J., Krzystek, P., Stilla, U., 2008. Analysis of full waveform LIDAR data for the classification of deciduous and coniferous trees. *International Journal of Remote Sensing*, 29 (5), pp. 1407-1431.
- Stenberg, P., Kangas, T., Smolander, H., Linder, S., 1999. Shoot structure, canopy openness and light interception in Norway spruce. *Plant, Cell and Environment*, 22, pp. 1133-1142.
- Stenberg, P., Kuuluvainen, T., Kellomäki, S., Grace, J.C., Jokela, E.J., Gholz, H.L., 1994: Crown structure, light interception and productivity of pine trees and stands. *Ecological Bulletins*, 43, pp. 20-34.
- Wagner, W., Ullrich, A., Ducic, V., Melzer, T., Studnicka, N., 2006. Gaussian decomposition and calibration of a novel small-footprint full-waveform digitising airborne laser scanner. *ISPRS Journal of Photogrammetry and Remote Sensing*, 60, pp. 100-112.
- Wagner, W., Hollaus, M., Briese, C. and Ducic, V., 2008. 3D vegetation mapping using small-footprint full-waveform airborne laser scanners. *International Journal of Remote Sensing*, 29(5), pp. 1433-1452.

6. ACKNOWLEDGEMENTS

The Hyttiälä field station's remote sensing experiment with abundant field reference data is a joint effort of personnel at Hyttiälä as well as the forestry students, researchers and teachers of the University of Helsinki who participated in the work 1995–2008. The aerial image and LiDAR datasets were made possible by funding from UPM-Kymmene, Metsämannut, Metsähallitus, Stora Enso, Blom-Kartta, Finnish Forest Research Institute, Finnish Geodetic Institute, Metsämiesten säätiö, University of Joensuu, and the University of Helsinki. Funding by Suomen luonnonvarain tutkimussäätiö, Academy of Finland and the University of Helsinki has enabled the research work.